Polyhedron 105 (2016) 246–252

Contents lists available at ScienceDirect

Polyhedron

journal homepage: www.elsevier.com/locate/poly

Copper(II) complexes of three isomeric bis(tacn) ligands: Syntheses, structures and properties

Campbell J. Coghlan [a,1], Eva M. Campi [a], Stuart R. Batten [b,c], W. Roy Jackson [a], Milton T.W. Hearn [a,*]

[a] Centre for Green Chemistry, Monash University, Clayton, Australia
[b] School of Chemistry, Monash University, Clayton, Australia
[c] Department of Chemistry, Faculty of Science, King Abdulaziz University, Jeddah, Saudi Arabia

ARTICLE INFO

Article history:
Received 1 October 2015
Accepted 1 December 2015
Available online 11 December 2015

Keywords:
Copper(II) complexes
Aza-macrocycles
Crystal structures
m-Xylene linkers
Immobilised metal ion affinity chromatography

ABSTRACT

Two new isomeric bis(tacn) ligands, 3,5-bis(1,4,7-triazacyclonon-1-ylmethyl)-1-(hydroxymethyl)-benzene (HL^{hyx}) and 2,6-bis(1,4,7-triazacyclonon-1-ylmethyl)anisole (L^{anx}) have been synthesised. In addition, 2,6-bis(1,4,7-triazacyclonon-1-ylmethyl)-4-methylphenol (HL^{ohx}) was also synthesised in a considerably higher yield than the previously reported method. The ligands were reacted with two equivalents of $Cu(NO_3)_2{\cdot}3H_2O$ at pH 5 resulting in the formation of three binuclear complexes. The ligands L^{anx} and HL^{hyx} form complexes $[Cu_2Cl_3(L)(H_2O)](PF_6)$ containing two unique Cu^{2+} centres coordinated to the ligand. In contrast, the phenolic HL^{ohx} ligand forms a bridged complex $[Cu_2(\mu\text{-}Cl)(L^{ohx})](PF_6)_2$, with the two Cu centres further linked by (μ-Cl) and (μ-O) bridges.

1. Introduction

The study of bis(tacn) ligands is a growing area of research and many different bridging groups have been synthesised [1–12]. Generally, these ligands have been synthesised using the orthoamide route first described by Zompa [13]. However, some ligands have been synthesised *via* different methods, such as tosyl protected bis(tacn) compounds [14,15] or through the Boc_2(tacn) intermediate [16]. The linker chain has been found to affect how the ligand binds to various metals. The effects range from forming polymeric cation compounds and dimers, to the formation of molecular sandwiches and intermolecular bridges [1–12].

Uses for these bis(tacn) ligands have included, but are not limited to, advanced modes of protein purification [17,18]. For example, these ligands have been used in immobilised metal affinity chromatography (IMAC) which has become a widely used method for protein purification. The technique relies upon a ligand being immobilised onto a solid support matrix and coordinated with a metal ion. The metal complex ideally then interacts with a peptide tag genetically engineered into to the protein of interest [19–22]. Typically, the tag consists of a short peptide chain with multiple metal-binding sites. The metal binding sites on the peptide chains arise from specific amino acid residues (e.g. histidine) which can coordinate to the metal ion in a manner similar to those bound to the bis(tacn) compound.

The interactions of bridged bis(tacn) ligands with borderline metal ions [23–25], such as Cu(II), Ni(II) or Zn(II), have been investigated previously [26–34]. Moreover, in our previous studies with various Cu^{2+} bis(tacn) complexes (as well as the corresponding complexes generated with Ni^{2+}, Zn^{2+} and other borderline metal ions), we demonstrated that when these complexes are used as immobilised ligands for the chromatographic purification of native and recombinant proteins, even closely related bridged bis(tacn) chelating compounds were found to behave differently in terms of their affinity binding constants (K_{assoc}s), binding capacities (Q_{max}s) or their on- and off-kinetics (k_{on}'s or k_{off}'s) associated with their interaction with native or recombinant proteins. These differences resulted in profound changes in performance between different members of this new class of immobilised metal ion affinity chromatographic (IMAC) resins for use in protein purification [35,36]. The current investigations were consequently designed to gain further insight into the origins of this behaviour through determination of the crystal structures of three such closely related *m*-xylene bridged Cu^{2+} bis(tacn) complexes and, in particular, determine the organisational arrangement around the Cu^{2+} ion(s) in these coordinated structures.

Potentially, the linker can have a large effect on how the metal can be coordinated. For example, we recently documented that bis(tacn) ligands bearing phenyl, carboxylic acid or nitro groups

* Corresponding author. Tel.: +61 3 9905 4547; fax: +61 3 9905 4597.
E-mail address: milton.hearn@monash.edu (M.T.W. Hearn).
[1] Current Address: School of Chemistry and Physics, Centre for Advanced Nanomaterials, The University of Adelaide, Adelaide 5005, Australia.

http://dx.doi.org/10.1016/j.poly.2015.12.004
0277-5387/

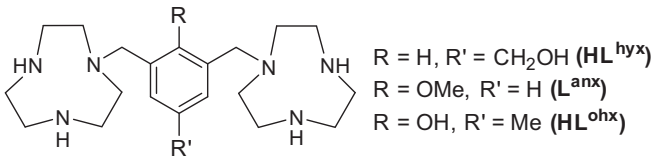

Fig. 1. Schematic representation and abbreviations of the bis(tacn) ligands.

on the bridging xylene ring give rise to copper(II) complexes with different and distinct crystalline structures [34]. This current paper reports on studies of how these new linkers, all containing aromatic rings bearing oxygen-containing substituents, affect the coordination of copper(II) metal ions. To this end, this study has focused on the synthesis of two new ligands, 3,5-bis(1,4,7-triazacyclonon-1-ylmethyl)-1-(hydroxy-methyl)-benzene (HL^{hyx}) (containing a CH_2OH group in the 1-position) and 2,6-bis(1,4,7-triazacyclonon-1-ylmethyl)anisole (L^{anx}) (containing an OMe group in the 1-position) and the known 2,6-bis(1,4,7-triazacyclonon-1-yl-methyl)-4-methylphenol (HL^{ohx}) (Fig. 1) using Boc_2tacn as the synthetic precursor. Following synthesis and characterisation of the bis(tacn) ligand products, the binding behaviour of these ligands with copper(II) ions was then investigated. It was anticipated that the metal–metal distances and metal binding characteristics of these macrocyclic complexes will give an indication of what may occur when these ligands are immobilised onto a solid support. Our objective was to ultimately establish the structural requirements necessary for these new metal–ligand complexes to exhibit enhanced binding to specifically tagged proteins during their downstream processing and purification from complex fermentation or cell culture feed-stocks. In addition, this study also highlights the benefits of employing the relatively underutilised Boc_2tacn as the precursor for the synthesis of these compounds and compares this alternative approach to the standard orthoamide route described by Zompa [13].

2. Results and discussion

The ligands HL^{hyx}, HL^{ohx} and L^{anx} were prepared (Scheme 1) using adaptations of a previously reported method described by Kimura and co-workers [37] for the synthesis of the analogous bridged cyclen compounds. The reaction of two equivalents of di-*tert*-butyl-1,4,7-triazonane-1,4-dicarboxylate (Boc_2tacn) with the appropriate substituted α,α′-dibromo-*m*-xylene reagent gave the corresponding Boc_4 bis(tacn) compound (Scheme 1). The Boc groups were removed with conc. HCl and the bis(tacn) compounds were isolated as their hydrochloride salts, L·6HCl. The bis(tacn) ligands HL^{hyx}, L^{anx} and HL^{ohx} were characterised by ^1H and ^{13}C NMR spectroscopy, mass spectrometry and elemental analysis. The previously reported HL^{ohx} hydrochloride salt had been prepared in a low yield (28%) from tacn orthoamide [38]. Using the methods discussed here, with Boc_2tacn as the starting material, the overall yield of the purified product was 74%, including the isolation of the intermediate Boc_4 bis(tacn) compound.

Each ligand (as the L·6HCl salt) was reacted with 2 equivalents of $Cu(NO_3)_2{\cdot}3H_2O$ in water, and the pH adjusted to approximately pH 5.0 with 4 M NaOH. This step was followed by the addition of the counter ion PF_6^- (as NH_4PF_6). The products crystallised from this mixture over several days and were characterised by X-ray crystallography and spectroscopic and analytical methods.

2.1. The structure of $[Cu_2(Cl)_3(L^{anx})(H_2O)](PF_6){\cdot}H_2O$ (**1**)

The asymmetric unit of **1** contains a binuclear Cu^{2+} complex cation (Fig. 2), a PF_6 counterion, and two intercalated water molecules (both with half occupancy). Within the complex there are two crystallographically- and chemically-distinct five-coordinate copper atoms; in addition to the tridentate tacn rings, the $Cu^{2+}(1)$ is coordinated by a chloride anion and a water molecule, whilst $Cu^{2+}(2)$ is coordinated by two chloride anions (Table 1). The ligand adopts a U-shaped geometry, with the tacn groups orientated in a divergent fashion, but with the metal atoms located on the same side of the ligand. The metal to metal distance within the complex is 10.315 Å. The aromatic methoxy substituent is not involved in any interactions.

Adjacent complexes are bound together through a series of hydrogen bonds (Table 2) between the Cl(1) and the N(6) hydrogen as well as hydrogen bonds between the Cl(2) and Cl(3) chlorine atoms with the O(1) hydrogen atoms as shown in Fig. 2B. These interactions and weaker N–H…Cl interactions (Table 2) link the complexes into 2D sheets that lie in a parallel (−101) plane. These sheets alternate with layers of PF_6 anions and intercalated water molecules. The intercalated water molecules form discrete hydrogen-bonded squares. Hydrogen bonds between these tetra-aqua squares, the PF_6 anions, the amine groups of the ligands, and the coordinated water molecules and chloride anions then link all these components into a complicated 3D network.

2.2. The structure of $[Cu_2(\mu\text{-}Cl)(L^{ohx})](PF_6)_2$ (**2**)

The asymmetric unit of **2** comprises a binuclear Cu^{2+} complex cation and two PF_6 counterions (Fig. 3). The tacn groups of the

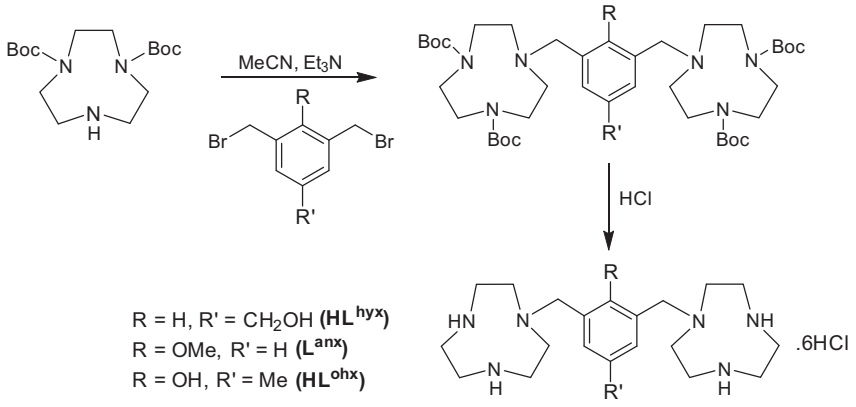

Scheme 1. Synthesis of the bis(tacn) ligands HL^{hyx}, L^{anx} and HL^{ohx}.

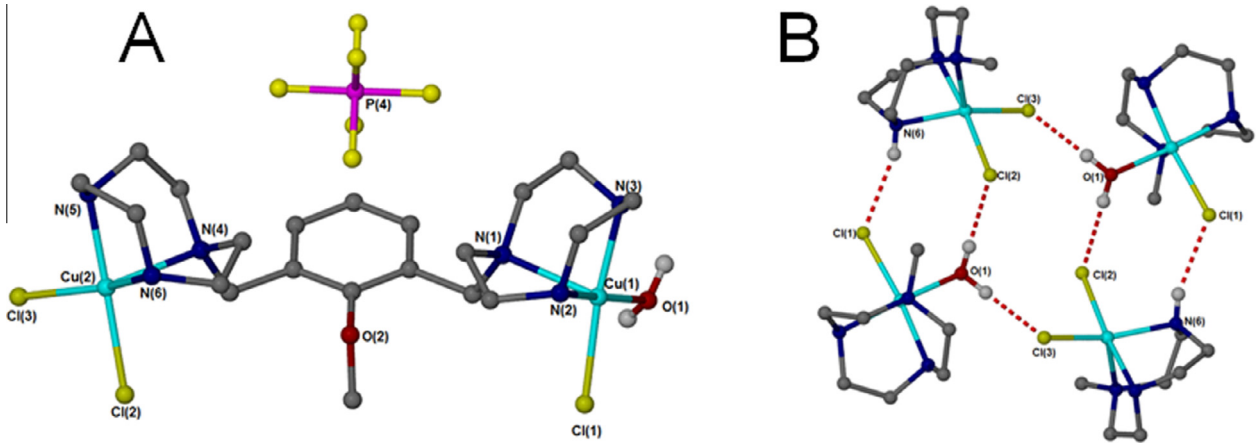

Fig. 2. Ball and stick representation of **1** (A) and the hydrogen bonding between complexes in **1** (B) (hydrogen bonds represented by dotted lines; some atoms omitted for clarity). Intercalated water molecules have also been omitted for clarity in both figures.

Table 1
Selected bond distances (Å) in compounds **1**, **2** and **3**.

	1	2	3
Cu(1)–N(1)	2.274(5)	2.031(2)	2.298(4)
Cu(1)–N(2)	2.011(5)	2.179(2)	2.017(5)
Cu(1)–N(3)	2.028(5)	1.999(2)	2.013(5)
Cu(2)–N(4)	2.286(5)	2.035(2)	2.281(4)
Cu(2)–N(5)	2.025(5)	2.192(2)	2.002(4)
Cu(2)–N(6)	2.045(5)	1.990(3)	2.035(5)
Cu(1)–Cl(1)	2.2790(17)	2.3134(8)	2.2679(18)
Cu(1)–Cl(2)	–	–	2.162(4)
Cu(1)–O(1)	2.010(4)	1.9427(19)	–
Cu(2)–Cl(2)	2.2942(18)	–	2.2501(16)
Cu(2)–Cl(3)	2.2484(18)	–	–
Cu(2)–O(1)	–	–	2.003(5)

Table 2[†]
Selected hydrogen bond distances (Å) and angles (°) in compounds **1**, **2** and **3**.

	D–H	H…A	D…A	D–H…A
1				
O(1)–H(1W)…Cl(3)^{I}	0.88(1)	2.21(2)	3.066(5)	164(5)
O(1)–H(2W)…Cl(2)^{II}	0.88(1)	2.29(1)	3.168(5)	176(6)
O(3)–H(4W)…O(4)^{III}	0.88(1)	2.40(11)	2.89(2)	116(9)
O(4)–H(6W)…O(3)^{IV}	0.88(1)	1.86(4)	2.72(2)	165(12)
O(4)–H(5W)…F(2)	0.88(1)	2.07(6)	2.86(1)	150(10)
N(5)–H(3N)…F(5)^{V}	0.87(2)	2.27(5)	3.022(7)	144(8)
N(2)–H(1N)…Cl(2)^{VI}	0.88(2)	2.54(4)	3.339(6)	152(6)
N(6)–H(4N)…Cl(1)^{VI}	0.87(2)	2.44(3)	3.278(5)	161(5)
N(3)–H(2N)…Cl(3)^{I}	0.89(2)	2.76(6)	3.406(5)	131(6)
2				
N(2)–H(2N)…F(1)	0.89(4)	2.46(4)	3.184(3)	139(3)
N(2)–H(2N)…F(5)	0.89(4)	2.57(4)	3.359(4)	147(3)
N(3)–H(3N)…F(11)^{I}	0.92(4)	2.09(4)	2.968(6)	161(3)
N(3)–H(3N)…F(16)^{I}	0.92(4)	2.22(4)	3.095(7)	160(3)
N(5)–H(5N)…F(4)^{II}	0.80(4)	2.28(4)	3.048(4)	162(4)
C(5)–H(5A)…F(2)^{I}	0.99	2.52	3.374(4)	144
3				
O(1)–H(1W)…O(5)	0.88(1)	1.87(1)	2.740(8)	169(2)
O(1)–H(2W)…O(2)^{I}	0.88(1)	1.86(1)	2.700(8)	159(2)
O(2)–H(2C)…O(4)	0.84	1.95	2.78(1)	169
O(3)…O(1)^{I}	–	–	3.18(1)	–
O(3)–H(4W)…O(5)	0.88(1)	2.38(1)	2.90(1)	118(2)
O(4)–H(5W)…F(4)^{II}	0.88(1)	2.40(13)	3.00(2)	126(13)
N(5)–H(5N)…O(2)^{III}	0.93	2.21	3.011(6)	143

[†] Symmetry operations: For **1**: I: $x-1/2, 3/2-y, z-1/2$; II: $1/2-x, y+1/2, 1/2-z$; III: $1-x, 1-y, -z$; IV: $x, y-1, z$; V: $3/2-x, y+1/2, 1/2-z$; VI: $1/2-x, y-1/2, 1/2-z$. For **2**: I: $1/3-y, x-y+2/3, z+2/3$; II: $y, y-x, -z$. For **3**: I: $1-x, 1-y, -z$; II: $x+1, y, z$; III: $x-1, y, z$.

ligand are orientated in a convergent fashion, bringing the metal ions close enough to be bridged by the oxygen substituent on the bridging central ring. The metals are further bridged by a chloride anion, leading to five-coordinate metal environments in which each copper atom is coordinated to three tacn amine atoms, a bridging phenoxy oxygen, and a chloride anion. The metal to metal distance is only 3.12 Å. The analogous Zn^{2+} complex has been reported recently [39]. Similar Cu^{2+} bis(tacn) complexes with a hydroxide bridge in place of the chloride [40], and an analogous manganese complex containing a pair of bridging acetates in place of the chloride [1,38], have also been reported. Unlike **1**, there is no obvious separation of the complexes and the PF_6^- counterions in the lattice. Furthermore, in the absence of the water molecules found in **1**, the most significant intermolecular interactions are hydrogen bonds between the amine groups of the ligand and the fluorines of the anions (Table 2). This hydrogen bonding connects the components into a complicated 3D network.

2.3. The structure of $[Cu_2(Cl)_3(HL^{hyx})(H_2O)](PF_6)\cdot 3H_2O$ (**3**)

As for the previous ligands, the hydroxymethyl ligand HL^{hyx} forms a dinuclear complex. The asymmetric unit of $[Cu_2(Cl)_3(HL^{hyx})(H_2O)](PF_6)\cdot 3H_2O$ (**3**) contains the dinuclear complex, one PF_6 counterion, and three lattice water molecules. As for **1**, the two five-coordinate copper atoms are different – in addition to the tacn ligand, Cu(1) binds to two chloride anions, while Cu(2) binds to one chloride and one water. Unlike **1**, however, the ligand adopts a Z-conformation, with complexes orientated on different sides of the ligand. The same conformation is seen in dinuclear copper complexes of very similar ligands [41,42]. In contrast, however, to related complexes of the L^{cax} [34] and the HL^{ohx} ligands, there is only a weak interaction between the copper(II) centre and an adjacent Cl(1) atom (3.085 Å). The metal to metal distance across the complex is 10.771 Å.

These complexes pack in hydrophobic layers dominated by the ligand backbone, which lie parallel to the (1 −1 0) plane. These layers alternate with hydrophilic layers of PF_6 counterions and intercalated water molecules. A chloride ligand bound to Cu(1), the coordinated water ligand on Cu(2), and the hydroxyl group of the ligand all project into this hydrophilic layer. Extensive hydrogen bonding (Table 2) between the coordinated and lattice water molecules, one of the ligand amine groups (N(5)), the ligand hydroxyl group, and one of the PF_6 fluorines (F(4)) link the components of the hydrophilic layers together (see Fig. 4).

In each of the three new complexes, the Cu coordination geometries are best described as square-based pyramidal, with the degree of distortion varying across the metal atoms. This is reflected in the τ values [43], which are 0.03 (Cu1) and 0.35 (Cu2) for **1**, 0.25 (Cu1) and 0.20 (Cu2) for **2**, and 0.01 (Cu1) and

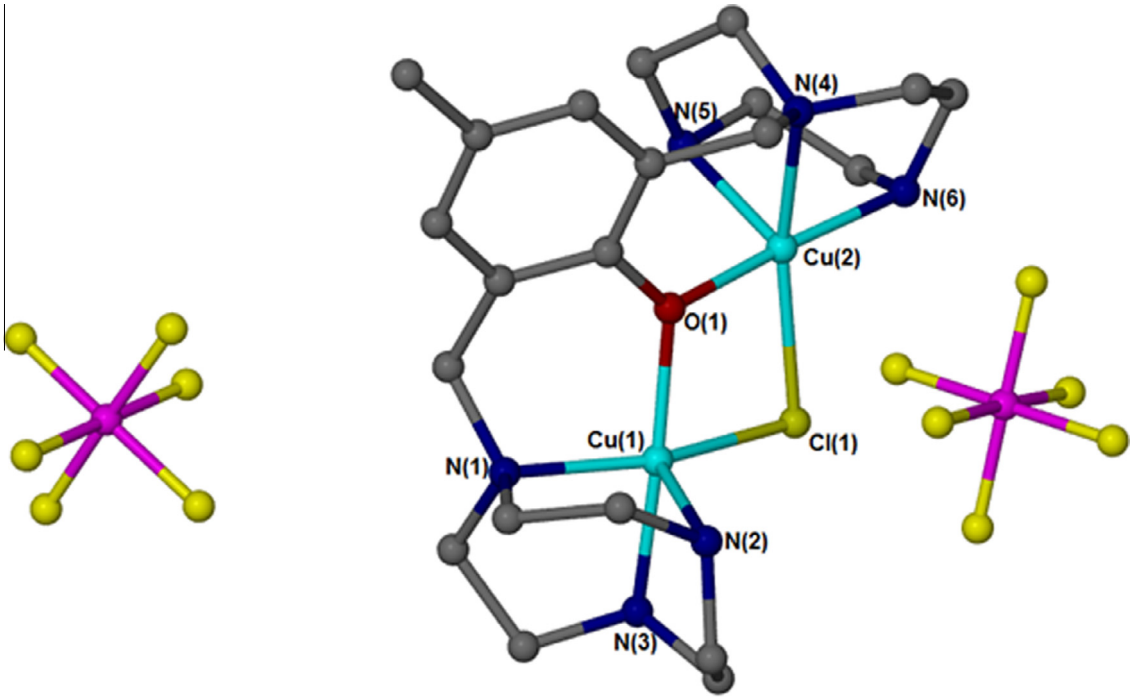

Fig. 3. Ball and stick representation of **2**. Some hydrogen atoms and the lattice water molecule have been omitted for clarity. One of the PF_6 anions is disordered over two positions, however only one position is shown for clarity.

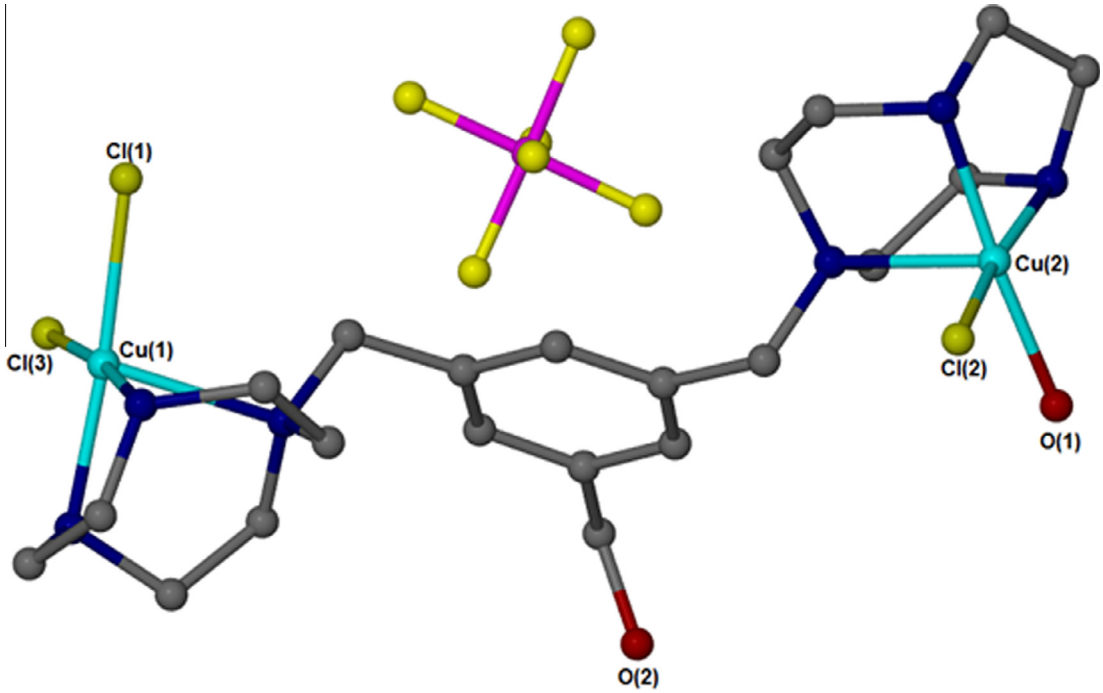

Fig. 4. Ball and stick representation of **3**; intercalated water omitted for clarity.

0.07 (Cu2) for **3**. A τ value of 0 indicates true square-based pyramidal geometry, while a value of 1 indicates trigonal bipyramidal geometry. The Cu—N bonds for complexes **1** and **3** are consistent with the general binding for bis(tacn) ligands, with the bond length to the tertiary amine in the apical position being slightly longer than the bond length to the secondary amines (Table 1). Complex **2** shows a shorter bond from Cu to the tertiary amine because of the bridging between the metal ions.

3. Conclusions

Three ligands HL^{hyx}, L^{anx}, and HL^{ohx} have been prepared and their binding to copper(II) investigated in this study. These results confirm that the functional group attached to the xylene linker has a significant influence on the nature of the crystallised product. The metal–metal distance in the solid state can vary from between 3.12 Å and 10.77 Å. Of particular interest is the observation that

the phenolic ligand HL^{ohx} is deprotonated and forms a μ-O and μ-Cl bridged structure whereas the alcohol in the related HL^{hyx} remains protonated and uncoordinated. The placing of the hydroxyl group in the 2-position of the central aromatic ring in HL^{ohx} is clearly the key; in HL^{hyx} the pendant alkoxy group is in the 5-position and binding to the tacn coordinated copper atoms is therefore more geometrically difficult. In L^{anx}, of course, the pendant group lacks a suitable donor atom to coordinate.

These results thus provide structural insights into the origins of the differences observed in the binding behaviour of recombinant proteins containing histidine-rich tags incorporated at the N-terminus of the target protein by recombinant DNA technologies, with bridged bis(tacn) ligands, such as the HL^{hyx}, L^{anx} and HL^{ohx} ligands, when these ligands are immobilised onto support materials and complexed with Cu(II) or other borderline metal ions to generate IMAC resins [35,36,44–46]. As an important experimental procedure in protein purification, many bi-, tri- and tetra-dentate chelating compounds have been employed with various borderline, e.g. Cu^{2+}, Ni^{2+}, Zn^{2+}, etc, or hard metal ions, e.g. Fe^{3+}, Al^{3+}, Yb^{2+}, etc, to generate IMAC adsorbents for use in protein purification. Despite their widespread use, detailed information on the structural requirements and geometries of the coordinated metal ion(s) within a specific chelated metal ion complex of the generated IMAC resins is frequently lacking. Thus, the need exists to establish better criteria to allow the selection of specific chelated metal ion complexes to achieve improved binding performance based on their structural complementarity to the primary and secondary structural features of the chosen histidine-rich tags. In this manner, the binding attributes of a specific IMAC resin, in terms of its K_{assoc}, Q_{max} and k_{on}/k_{off}, can be optimised. The current investigation related to the arrangement of the coordinated Cu^{2+} centres present within the three closely related bis(tacn) chelating ligands, thus provides knowledge relevant to these considerations. In particular, when each of these xylene-bridged bis(tacn) ligands was immobilised onto the support gel, Sepharose 6 FF™, the protein binding performance of the derived IMAC resins in batch (static) and dynamic binding modes with the hexa-histidine tagged green fluorescent protein (His6-GFP) and hexa-histidine tagged glutathione S-transferase (His6-GST), revealed significant differences. For example, the IMAC resin derived from the HL^{ohx} (phenolic) ligand, in contrast to the other two bridged xylene-based bis(tacn) IMAC resins, exhibited very weak binding with His6-GFP and none with His6-GST. These findings is consistent with the steric hindrance observed around the coordinated Cu^{2+} ion in the crystal structure of the corresponding Cu^{2+}–HL^{ohx} complex, an effect which would prevent binding of a histidine-rich tag to the coordinated Cu^{2+} ion.

4. Experimental

Reagent or analytical grade materials were obtained from commercial suppliers and used without further purification. ^1H and ^{13}C NMR spectra were recorded on either a Bruker DPX 300 or a Bruker DPX 400 spectrometer. The NMR spectra were recorded as solutions in base washed $CDCl_3$, D_2O or d_6-DMSO and are reported relative to TMS (tetramethylsilane δ 0.00 ppm). Low resolution electrospray ionisation mass spectra (ESI) were recorded on a Micromass Platform ll API QMS Electrospray mass spectrometer and all samples were run in methanol unless otherwise indicated. The samples were run in positive $(ESI)^+$ mode. Microanalysis of samples sealed in glass ampoules under nitrogen were determined by the Campbell Microanalytical Service at the University of Otago, New Zealand. Boc_2tacn was synthesised according literature preparation methods and the NMR data were consistent with literature data [16]. 3,5-Bis(bromomethyl)benzyl alcohol was prepared by DIBAL-H reduction [47] of methyl 3,5-bis(bromomethyl)benzoate.

4.1. General method for formation of Boc_4-bis(tacn) compounds

Triethylamine (20 mmol) and the substituted α,α′-dibromo-*m*-xylene (8 mmol) were added to a solution of Boc_2 tacn (16 mmol) in CH_3CN (100 mL) and the mixture was stirred for 3 days at reflux. The mixture was concentrated to a dark amber gum which was dissolved in CH_2Cl_2 (50 mL) and washed consecutively with 10% aq. NaOH (2 × 50 mL), H_2O (50 mL), and brine (50 mL). The aqueous phases were combined and back extracted with CH_2Cl_2 (2 × 20 mL). The combined organic layers were concentrated to an amber gum which was redissolved in CH_2Cl_2 (4 mL) and chromatographed on a plug of silica (EtOAc/hexanes, 1:1 → 2:1) to give the Boc protected bis(tacn) compound.

4.2. 1,4-Di-tert-butyl-7,7′-(4-methylphenol-2,6-diyl)bis(1,4,7-triazonane-1,4-dicarboxylate)

Reaction of triethylamine (2 mL), 2,6-bis(bromomethyl)-4-methylphenol (3.00 g, 10 mmol) and Boc_2tacn (7.92 g, 21 mmol) in CH_3CN (100 mL) as described above gave the target compound as a yellow oil. Yield 6.98 g (85%). ^1H NMR (400 MHz, $CDCl_3$), δ (ppm): 1.49 (36H, m, CH_3), 2.04 (3H, s, $ArCH_3$), 2.70 (8H, m, tacn CH_2), 3.31 (8H, m, tacn CH_2), 3.47 (8H, m, tacn CH_2), 3.73 (4H, s, $ArCH_2$), 6.86 (2H, m, ArH). ^{13}C NMR (100 MHz, $CDCl_3$), δ (ppm): 20.6 (CH_3), 28.6 (CH_3), 49.6 (tacn CH_2), 50.3 (tacn CH_2), 53.0 (tacn CH_2), 57.1 (CH_2), 79.8 (ArC), 153.7 (ArC), 155.3 (ArCH), 153.2 (ArC), 155.4 (ArC), 155.6 (C═O). ESI-MS *m*/*z* 791.4 $[M+H]^+$.

4.3. 1,4-Di-tert-butyl-7,7′-(1-(hydroxymethyl)benzene-3,5-diyl)bis(1,4,7-triazonane-1,4-dicarboxylate)

The reaction of triethylamine (1 mL), 3,5-bis(bromomethyl) benzyl alcohol (1.50 g, 5 mmol) and Boc_2tacn (3.17 g, 10 mmol) in CH_3CN (60 mL) as described above gave the target compound as a yellow oil. Yield 2.77 g (68%). ^1H NMR (400 MHz, $CDCl_3$), δ (ppm): 1.45 (36H, m, CH_3), 2.70 (8H, m, tacn CH_2), 3.24 (8H, m, tacn CH_2), 3.47 (8H, m, tacn CH_2), 3.70 (4H, s, $ArCH_2$), 4.67 (2H, s, CH_2OH), 7.10 (1H, m, ArH). 7.3 (2H, m, ArH). ^{13}C NMR (100 MHz, $CDCl_3$), δ (ppm): 28.6 (CH_3), 49.8 (tacn CH_2), 50.5 (tacn CH_2), 54.6 (tacn CH_2), 60.4 ($ArCH_2$), 61.6 (CH_2OH), 79.5 (ArC), 125.8 (ArCH), 128.4 (ArCH), 140.0 (ArC), 143.6 (ArC), 155.7 (C═O). ESI-MS *m*/*z* 791.4 $[M+H]^+$.

4.4. 1,4-Di-tert-butyl-7,7′-(anisole-2,6-diyl)bis(1,4,7-triazonane-1,4-dicarboxylate)

The reaction of triethylamine (1 mL), 2,6-bis(bromomethyl)anisole [48] (2.50 g, 8 mmol) and Boc_2tacn (5.66 g, 20 mmol) in CH_3CN (100 mL) as described above gave the target compound as a yellow oil. Yield 5.55 g (81%). ^1H NMR (400 MHz, $CDCl_3$), δ (ppm): 1.40 (36H, m, CH_3), 2.70 (8H, m, tacn CH_2), 3.28 (8H, m, tacn CH_2), 3.51 (8H, m, tacn–CH_2), 3.70 (3H, s, OCH_3), 3.74 (4H, s, $ArCH_2$), 7.40 (1H, m, ArH). 7.48 (2H, m, ArH). ^{13}C NMR (100 MHz, $CDCl_3$), δ (ppm): 28.5 (CH_3), 49.3 (tacn CH_2), 49.7 (tacn CH_2), 50.3 (tacn CH_2), 53.2 ($ArCH_2$), 53.9 (OCH_3), 79.5 (ArC), 131.0 (ArCH), 132.3 (ArC), 155.5 (ArCH), 155.7 (C═O), 157.0 (C—O). ESI-MS *m*/*z* 791.4 $[M+H]^+$.

4.5. General method for formation of bis(tacn) salts

The Boc protected bis(tacn) compound (3 mmol) was dissolved in conc. HCl (50 mL) and the mixture stirred for 12 h at ambient temperature. The solution was concentrated under reduced

pressure and the precipitate collected by filtration and washed with cold absolute EtOH (50 mL) to give the HCl salt of the bis(tacn) compound.

4.6. 3,5-Bis(1,4,7-triazacyclonon-1-ylmethyl)-1-(hydroxymethyl) benzene·6HCl·4H_2O, (HL^{hyx}·6HCl·salt)

1,4-Di-*tert*-butyl-7,7′-(1-(hydroxymethyl)benzene-3,5-diyl)bis (1,4,7-triazonane-1,4-dicarboxylate) (2.77 g, 3 mmol) was dissolved in conc. HCl (50 mL) and the mixture stirred for 12 h as described above. The 6HCl salt of HL^{hyx} was isolated as a white solid. Yield 1.54 g (71%). ^{1}H NMR (400 MHz, D_2O), δ (ppm): 3.06 (8H, m, tacn CH_2), 3.28 (8H, m, tacn CH_2), 3.68 (8H, s, tacn CH_2), 3.98 (4H, s, CH_2Ar), 4.71 (2H, s, ArCH_2), 7.40 (1H, s, ArH), 7.46 (2H, s, ArH). ^{13}C NMR (100 MHz, D_2O), δ (ppm): 42.2 (tacn CH_2), 43.7 (tacn CH_2), 47.4 (tacn CH_2), 58.4 (ArCH_2), 63.4 (CH_2OH), 121.4 (ArCH), 128.8 (ArC), 131.5 (ArCH), 136.2 (ArC), Selected IR bands (cm^{-1}): 3357br vs, 2963vs, 2660br vs, 1724s, 1444s, 1161br s, 1111s, 1077s, 876s, 764s. ESI-MS *m*/*z* 390.3 [M+H]$^+$. *Anal.* Calc. for $C_{21}H_{52}Cl_6N_6O_5$ (HL^{hyx}·6HCl·4H_2O): C, 37.0; H, 7.7; N, 12.3. Found: C, 37.1; H, 7.1; N, 11.8%.

4.7. 2,6-Bis(1,4,7-triazacyclonon-1-ylmethyl)anisole·6HCl·3.5H_2O, (L^{anx}·6HCl salt)

1,4-Di-*tert*-butyl-7,7′-(anisole-2,6-dyl)bis(1,4,7-triazonane-1,4-dicarboxylate) (5.55 g, 7 mmol) was dissolved in conc. HCl (50 mL) and the mixture stirred for 12 h as described above. The 6HCl salt of L^{anx} was isolated as a white solid. Yield 3.90 g (90%). ^{1}H NMR (400 MHz, D_2O), δ (ppm): 2.94 (8H, m, tacn CH_2), 3.18 (8H, m, tacn CH_2), 3.46 (8H, s, tacn CH_2), 3.86 (3H, s, CH_3), 3.86 (4H, s, CH_2Ar), 7.08 (1H, m, ArH), 7.30 (2H, m, ArH). ^{13}C NMR (100 MHz, D_2O), δ (ppm): 41.5 (tacn CH_2), 42.7 (tacn CH_2), 46.8 (tacn CH_2), 52.5 (ArCH_2), 62.7 (OCH_3), 125.2 (ArCH), 128.0 (ArC), 132.9 (ArCH), 157.7 (ArC). Selected IR bands (cm^{-1}): 3369br vs, 2961vs, 2659br vs, 1583s, 1498s, 1433br s, 1257s, 1216s, 990s, 822s. ESI-MS *m*/*z* 390.3 [M+H]$^+$. *Anal.* Calc. for $C_{21}H_{51}Cl_6N_6O_{4.5}$ (L^{anx}·6HCl·3·5H_2O): C, 37.5; H, 7.6; N, 12.5. Found: C, 37.4; H, 7.6; N, 12.4%.

4.8. 2,6-Bis(1,4,7-triazacyclonon-1-ylmethyl)-4-methylphenol· 6HCl·4H_2O, (HL^{ohx}·6HCl salt)

1,4-Di-*tert*-butyl-7,7′-(4-methylphenol-2,6-diyl)bis(1,4,7-triazonane-1,4-dicarboxylate) (6.98 g, 9 mmol) was dissolved in conc. HCl (100 mL) and the mixture stirred for 12 h as described above. The HCl salt of HL^{ohx} was isolated as a white solid. Yield 5.19 g (92%). ^{1}H NMR (400 MHz, D_2O), δ (ppm): 2.32 (3H, s, CH_3), 3.08 (8H, m, tacn CH_2), 3.28 (8H, m, tacn CH_2), 3.66 (8H, s, tacn CH_2), 3.98 (4H, s, CH_2Ar), 7.26 (2H, s, ArH). ^{13}C NMR (100 MHz, D_2O), δ (ppm): 19.5 (CH_3), 42.5 (tacn CH_2), 44.1 (tacn CH_2), 48.1 (tacn CH_2), 54.1 (ArCH_2), 124.6 (ArCH), 131.7 (ArC), 132.9 (ArCH), 150.5 (ArC). Selected IR bands (cm^{-1}): 3368br vs, 2960vs, 2654br vs, 1582s, 1499s, 1426br s, 1111s, 1009s, 764s, 699s. ESI-MS *m*/*z* 390.3 [M+H]$^+$. *Anal.* Calc. for $C_{21}H_{52}Cl_6N_6O_5$ (HL^{ohx}·6HCl·4H_2O): C, 37.0; H, 7.7; N, 12.3. Found: C, 37.1; H, 7.1; N, 11.8%. The NMR data were consistent with literature data [38].

4.9. [$Cu_2(Cl)_3(L^{anx})(H_2O)$]($PF_6$)·$H_2O$ (**1**)

$Cu(NO_3)_2$·3H_2O (0.08 g, 0.32 mmol) and L^{anx}·6HCl (0.10 g, 0.16 mmol) were dissolved in H_2O (10 mL). The pH of the solution was adjusted to pH 5.0 with 4 M NaOH and the mixture stirred for 20 min. Ammonium hexafluorophosphate (0.08 g, 0.48 mmol) was added and the solution was left to slowly evaporate overnight followed by filtration to remove a precipitate. The solution was left to evaporate over a number of days to yield blue crystals. The solid was collected by filtration and washed quickly with a small amount of cold H_2O. Yield 0.10 g (76%). Selected IR bands (cm^{-1}): 3636s, 3318s 3268s, 3244s, 3210s, 2946br s, 2860br s,1617br s, 1584br s, 1527s, 1489s, 1455s, 1350s, 1280s, 1243s, 1148s, 1094vs, 1039vs, 1010s, 822vs, 782s, 697s. *Anal.* Calc. for $C_{21}H_{42}Cl_3Cu_2F_6N_6O_3P$ ([$Cu_2(Cl)_3(L^{anx})(H_2O)$]($PF_6$)·$H_2O$): C, 31.3; H, 5.3; N, 10.4. Found: C, 31.4; H, 5.1; N, 10.5%.

4.10. [$Cu_2(\mu$-Cl)(L^{ohx})](PF_6)$_2$ (**2**)

$Cu(NO_3)_2$·3H_2O (0.08 g, 0.34 mmol) and HL^{ohx}·6HCl (0.10 g, 0.17 mmol) were dissolved in H_2O (10 mL). The pH of the solution was adjusted to pH 5.0 with 4 M NaOH and the mixture stirred for 20 min. Ammonium hexafluorophosphate (0.08 g, 0.48 mmol) was added and the solution was left to slowly evaporate overnight followed by filtration to remove a precipitate. The solution was left to evaporate over a number of days to yield green crystals. The solid was collected by filtration and washed quickly with a small amount of cold H_2O. Yield 0.13 g (87%). Selected IR bands (cm^{-1}): 3635s, 3372 m, 3320s, 2864br s, 2084br s, 1890br, w, 1578s, 1527s, 1488vs, 1468s, 1347s, 1318s, 1278vs, 1255s, 1166s, 1147s, 1095s, 1083vs, 1026vs, 1008vs, 954vs, 925s, 827vs, 738s, 659s. *Anal.* Calc. for $C_{21}H_{37}ClCu_2F_{12}N_6O_1P_2$ ([Cu_2(Cl)(L^{ohx})](PF_6)$_2$): C, 30.0; H, 4.4; N, 10.0. Found: C, 30.7; H, 4.6; N, 9.8%.

4.11. [$Cu_2(Cl)_3(HL^{hyx})(H_2O)$]($PF_6$)·3$H_2O$ (**3**)

$Cu(NO_3)_2$·3H_2O (0.08 g, 0.32 mmol) and HL^{hyx}·6HCl (0.10 g, 0.16 mmol) were dissolved in H_2O (10 mL). The pH of the solution was adjusted to pH 5.0 with 4 M NaOH and the mixture stirred for 20 min. Ammonium hexafluorophosphate (0.08 g, 0.48 mmol) was added and the solution was left to slowly evaporate overnight followed by filtration to remove a precipitate. The solution was left to evaporate over a number of days to yield blue crystals. The solid was collected by filtration and washed quickly with a small amount of cold H_2O. Yield 0.13 g (94%). Selected IR bands (cm^{-1}): 3327s, 3238br s, 2930s, 2874s, 2113br w, 1605w, 1488s, 1453s, 1355s, 1296s, 1235s, 1168w, 1093s, 1010br s, 947s, 829vs, 739s. *Anal.* Calcd for $C_{21}H_{42}Cl_3Cu_2F_6N_6O_3P$ ([$Cu_2Cl_3(HL^{hyx})H_2O$](PF_6)· H_2O): C, 31.3; H, 5.5; N, 10.4. Found: C, 31.1; H, 5.1; N, 10.7%.

4.12. Crystal structure determinations

Only very small crystals for compounds **1**, **2** and **3** were obtained. Consequently data for each were measured using the MX1 beamline at the Australian Synchrotron, Victoria Australia. The end station comprised a φ goniostat with a Quantum 210r area detector and data were collected at a single wavelength (λ = 0.71068 Å) using the Blue Ice GUI [49] and processed using the XDS software.[50] Due to hardware constraints (fixed detector angle, minimum detector distance) the maximum obtainable resolution at the detector edge was approximately 0.83 Å. All structures were solved by standard methods and refined by full matrix least squares on F^2 (SHELX-97) [51] with anisotropic displacement parameter forms for non-hydrogen atoms. Plausible positions of hydrogen atoms attached to N or O were located in the difference Fourier map and were refined with N–H/O–H distances restrained to reasonable values (0.88–0.98 Å); all other hydrogen atoms were placed in calculated positions and constrained to ride on the parent atoms with U_{iso}(H) = 1.2.U_{eq}(C).

4.12.1. Crystal and refinement data

1 $C_{21}H_{42}Cl_3Cu_2F_6N_6O_3P$, M = 805.01, blue prism, 0.03 × 0.02 × 0.02 mm^3, monoclinic, space group $P2_1/n$ (No. 14), a = 13.996(3), b = 8.5970(17), c = 26.909(5) Å, β = 99.83(3)°, V = 3190.2(11) Å^3, Z = 4, D_c = 1.676 g/cm^3, F_{000} = 1648, goniostat with quantum 210r

detector, synchrotron radiation, $\lambda = 0.71068$ Å, $T = 100(2)$K, $2\theta_{max} = 53.3°$, 45021 reflections collected, 6631 unique ($R_{int} = 0.1442$). Final *GooF* = 1.023, $R_1 = 0.0640$, $wR_2 = 0.1510$, *R* indices based on 4202 reflections with $I > 2\sigma(I)$ (refinement on F^2), 423 parameters, 13 restraints. Lp and absorption corrections applied, $\mu = 1.699$ mm^{-1}.

2 $C_{21}H_{37}ClCu_2F_{12}N_6OP_2$, $M = 842.04$, blue rectangular, $0.04 \times 0.03 \times 0.02$ mm^3, trigonal, space group *R*-3 (No. 148), $a = b = 35.660(5)$, $c = 13.209(3)$ Å, $V = 14547(4)$ Å^3, $Z = 18$, $D_c = 1.730$ g/cm^3, $F_{000} = 7668$, goniostat with quantum 210r detector, synchrotron radiation, $\lambda = 0.71068$ Å, $T = 100(2)$ K, $2\theta_{max} = 53.8°$, 36055 reflections collected, 6762 unique ($R_{int} = 0.0378$). Final *GooF* = 1.059, $R_1 = 0.0417$, $wR_2 = 0.1160$, *R* indices based on 6363 reflections with $I > 2\sigma(I)$ (refinement on F^2), 459 parameters, 0 restraints. Lp and absorption corrections applied, $\mu = 1.595$ mm^{-1}.

3 $C_{21}H_{46}Cl_3Cu_2F_6N_6O_5P$, $M = 841.04$, blue prism, $0.30 \times 0.20 \times 0.10$ mm^3, triclinic, space group $P\bar{1}$ (No. 2), $a = 11.440(2)$, $b = 12.180(2)$, $c = 14.490(3)$ Å, $\alpha = 72.05(3)$, $\beta = 69.19(3)$, $\gamma = 80.11(3)°$, $V = 1791.1(6)$ Å^3, $Z = 2$, $D_c = 1.556$ g/cm^3, $F_{000} = 860$, goniostat with quantum 210r detector, synchrotron radiation, $\lambda = 0.71068$ Å, $T = 100(2)$ K, $2\theta_{max} = 55.0°$, 29199 reflections collected, 7554 unique ($R_{int} = 0.0417$). Final *GooF* = 1.038, $R_1 = 0.0907$, $wR_2 = 0.2667$, *R* indices based on 6839 reflections with $I > 2\sigma(I)$ (refinement on F^2), 415 parameters, 71 restraints. Lp and absorption corrections applied, $\mu = 1.521$ mm^{-1}.

The completeness of this structure is low due to the constraints of using the goniometer (phi rotation) while utilising the synchrotron radiation source. Multiple attempts to collect data were undertaken however due to the small nature of crystal better data could not be obtained.

Acknowledgements

Part of this research was carried out on the MX1 beamline at the Australian Synchrotron, Victoria, Australia. Financial support from Novo Nordisk A/S and from the Australian Research Council for Linkage Grant funding which included a scholarship (to C.J.C.) is gratefully acknowledged.

Appendix A. Supplementary data

CCDC 1003839, 1003840 and 1003674 contains the supplementary crystallographic data for compound **1**, **2** and **3** respectively. These data can be obtained free of charge via http://www.ccdc.cam.ac.uk/conts/retrieving.html, or from the Cambridge Crystallographic Data Centre, 12 Union Road, Cambridge CB2 1EZ, UK; fax: (+44) 1223-336-033; or e-mail: deposit@ccdc.cam.ac.uk.

References

[1] H.R. Chang, H. Diril, M.J. Nilges, X. Zhang, J.A. Potenza, H.J. Schugar, D.N. Hendrickson, S.S. Isied, J. Am. Chem. Soc. 110 (1988) 625.
[2] B. Graham, G.F. Fallon, M.T.W. Hearn, D.C.R. Hockless, G. Lazarev, L. Spiccia, Inorg. Chem. 36 (1997) 6366.
[3] L.J. Farrugia, P.A. Lovatt, R.D. Peacock, J. Chem. Soc., Dalton Trans. (1997) 911.
[4] J.L. Sessler, J.W. Sibert, A.K. Burrell, V. Lynch, J.T. Markert, C.L. Wooten, Inorg. Chem. 32 (1993) 4277.
[5] N. Tanaka, Y. Kobayashi, S. Takamoto, Chem. Lett. (1977) 107.
[6] K. Wieghardt, I. Tolksdorf, W. Herrmann, Inorg. Chem. 24 (1985) 1230.
[7] J.L. Sessler, J.W. Sibert, V. Lynch, Inorg. Chem. 29 (1990) 4143.
[8] J.L. Sessler, J.W. Sibert, A.K. Burrell, V. Lynch, J.T. Markert, C.L. Wooten, Inorg. Chem. 32 (1993) 621.
[9] X. Zhang, W.-Y. Hsieh, T.N. Margulis, L.J. Zompa, Inorg. Chem. 34 (1995) 2883.
[10] D. Hanke, K. Wieghardt, B. Nuber, R.S. Lu, R.K. McMullan, T.F. Koetzle, R. Bau, Inorg. Chem. 32 (1993) 4300.
[11] M.J. Young, J. Chin, J. Am. Chem. Soc. 117 (1995) 10577.
[12] L. Tang, J. Park, H.-J. Kim, Y. Kim, S.J. Kim, J. Chin, K.M. Kim, J. Am. Chem. Soc. 130 (2008) 12606.
[13] L.J. Zompa, Inorg. Chem. 17 (1978) 2531.
[14] S. Pulacchini, M. Watkinson, Eur. J. Org. Chem. 22 (2001) 4233.
[15] S. Pulacchini, K. Shastri, N.C. Dixon, M. Watkinson, Synthesis 16 (2001) 2381.
[16] O. Iranzo, T. Elmer, J.P. Richard, J.R. Morrow, Inorg. Chem. 42 (2003) 7737.
[17] W. Jiang, B. Graham, L. Spiccia, M.T.W. Hearn, Anal. Biochem. 255 (1998) 47.
[18] B. Graham, M.T.W. Hearn, L. Spiccia, B.W. Skelton, A.H. White, Aust. J. Chem. 56 (2003) 1259.
[19] E. Hochuli, W. Bannwarth, H. Döbeli, R. Gentz, D. Stüber, Nat. Biotechnol. 6 (1988) 1321.
[20] R. Gutiérrez, E.M. Martín del Valle, M.A. Galán, Sep. Purif. Rev. 36 (2007) 71.
[21] E.S. Hemdan, Y. Zhao, E. Sulkowski, J. Porath, Proc. Natl. Acad. Sci. U.S.A. 86 (1989) 1811.
[22] J.T. Mooney, D.P. Fredericks, M.T.W. Hearn, Sep. Purif. Technol. 120 (2013) 265.
[23] R.G. Pearson, J. Chem. Educ. 45 (1968) 581.
[24] K.L. Haas, K.J. Franz, Chem. Rev. 109 (2009) 4921.
[25] E. Nieboer, D.H.S. Richardson, Environ. Pollut. B 1 (1980) 3.
[26] F.H. Fry, L. Spiccia, P. Jenson, B. Moubaraki, K.S. Murray, R.T. Tiekink, Inorg. Chem. 42 (2003) 5594.
[27] B. Graham, M.J. Grannas, M.T.W. Hearn, C.M. Kepert, L. Spiccia, B.W. Skelton, A. H. White, Inorg. Chem. 39 (2000) 1092.
[28] B. Graham, L. Spiccia, A.M. Bond, M.T.W. Hearn, C.M. Kepert, J. Chem. Soc., Dalton Trans. (2001) 2232.
[29] B. Graham, L. Spiccia, B.W. Skelton, A.H. White, D.C.R. Hockless, Inorg. Chim. Acta 358 (2005) 3974.
[30] M.J. Belousoff, B. Graham, B. Moubaraki, K.S. Murray, L. Spiccia, Eur. J. Org. Chem. 42 (2006) 4872.
[31] S.J. Brudenell, L. Spiccia, A.M. Bond, P.C. Mahon, D.C.R. Hockless, J. Chem. Soc., Dalton Trans. (1998) 3919.
[32] F.H. Fry, G.D. Fallon, L. Spiccia, Inorg. Chim. Acta 346 (2003) 57.
[33] T. Moufarrej, K. Bui, L.J. Zompa, Inorg. Chim. Acta 340 (2002) 56.
[34] C.J. Coghlan, E.M. Campi, C.M. Forsyth, W.R. Jackson, M.T.W. Hearn, Polyhedron 69 (2014) 219.
[35] J.T. Mooney, D.P. Fredericks, C. Zhang, T. Christensen, C. Jespergaard, C.B. Schiødt, M.T.W. Hearn, Prot. Express. Purif. 94 (2014) 85.
[36] C. Zhang, D.P. Fredericks, D. Longford, E.M. Campi, T. Sawford, M.T.W. Hearn, Biotechnol. J. 10 (2015) 480.
[37] E. Kimura, S. Aoki, T. Koike, M. Shiro, J. Am. Chem. Soc. 119 (1997) 3068.
[38] H. Diril, H.R. Chang, M.J. Nilges, X. Zhang, J.A. Potenza, H.J. Schugar, S.S. Isied, D. N. Hendrickson, J. Am. Chem. Soc. 111 (1989) 5102.
[39] D. Montagner, V. Gandin, C. Marzano, A. Erxleben, Eur. J. Inorg. Chem. (2014) 4084.
[40] D. Montagner, V. Gandin, C. Marzano, A. Erxleben, J. Inorg. Biochem. 145 (2015) 101.
[41] S. Mahapatra, S. Kaderli, A. Llobet, Y. Neuhold, T. Palanché, J.A. Halfen, V.G. Young, T.A. Kaden, L. Que, A.D. Zuberbühler, W.B. Tolman, Inorg. Chem. 36 (1997) 6343.
[42] H.-J. Wang, C.-T. Wu, B.-S. Luo, Chin. J. Struct. Chem. 17 (1998) 119.
[43] A.W. Addison, T.N. Rao, J. Reedijk, J. van Rijn, G.C. Verschoor, J. Chem. Soc., Dalton Trans. (1984) 1349.
[44] M. Petzold, C.J. Coghlan, M.T.W. Hearn, J. Chromatogr. A 1351 (2014) 61.
[45] C.J. Coghlan, E.M. Campi, C.M. Forsyth, W.R. Jackson, M.T.W. Hearn, Aust. J. Chem. 68 (2014) 1115.
[46] M.T.W. Hearn, in: S. Ahuja (Ed.), Handbook of Bioseparation, Academic Press, San Diego, 2000, pp. 72–235.
[47] M. Kathiresan, L. Walder, F. Ye, H. Reuter, Tetrahedron Lett. 51 (2010) 2188.
[48] T. Routasalo, J. Helaja, J. Kavakka, A.M.P. Koskinen, Eur. J. Inorg. Chem. (2008) 3190.
[49] T.M. McPhillips, S.E. McPhillips, H.J. Chiu, A.E. Cohen, A.M. Deacon, P.J. Ellis, E. Garman, A. Gonzalez, N.K. Sauter, R.P. Phizackerley, S.M. Soltis, P. Kuhn, J. Synchrotron Rad. 9 (2002) 401.
[50] W.J. Kabsch, J. Appl. Cryst. 26 (1993) 795.
[51] SHELX-97, SADABS, G.M. Sheldrick, Acta Crystallogr., Sect. A 64 (2008) 112.